Accepted Manuscript

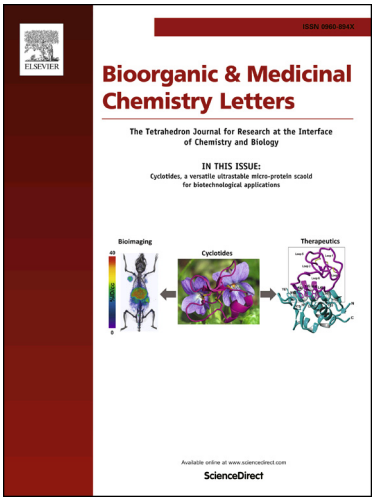

Identification of second-generation P2X3 antagonists for treatment of pain

Anthony Ginnetti, Daniel Paone, Shaun Stauffer, Craig Potteiger, Anthony Shaw, James Deng, James Mulhearn, Diem Nguyen, Carolyn Segerdell, Juliana Anquandah, Amy Calamari, Gong Cheng, Michael Leitl, Annie Liang, Eric Moore, Jacqueline Panigel, Mark Urban, Jixin Wang, Kerry Fillgrove, Cuyue Tang, Sean Cook, Stefanie Kane, Christopher Salvatore, Samuel Graham, Christopher Burgey

PII: S0960-894X(18)30144-6
DOI: https://doi.org/10.1016/j.bmcl.2018.02.039
Reference: BMCL 25635

To appear in: *Bioorganic & Medicinal Chemistry Letters*

Received Date: 5 January 2018
Revised Date: 15 February 2018
Accepted Date: 19 February 2018

Please cite this article as: Ginnetti, A., Paone, D., Stauffer, S., Potteiger, C., Shaw, A., Deng, J., Mulhearn, J., Nguyen, D., Segerdell, C., Anquandah, J., Calamari, A., Cheng, G., Leitl, M., Liang, A., Moore, E., Panigel, J., Urban, M., Wang, J., Fillgrove, K., Tang, C., Cook, S., Kane, S., Salvatore, C., Graham, S., Burgey, C., Identification of second-generation P2X3 antagonists for treatment of pain, *Bioorganic & Medicinal Chemistry Letters* (2018), doi: https://doi.org/10.1016/j.bmcl.2018.02.039

Identification of second-generation P2X3 antagonists for treatment of pain

Anthony Ginnetti[a], Daniel Paone[a], Shaun Stauffer[a], Craig Potteiger[a], Anthony Shaw[a], James Deng[a], James Mulhearn[a], Diem Nguyen[a], Carolyn Segerdell[a], Juliana Anquandah[b], Amy Calamari[b], Gong Cheng[b], Michael Leitl[b], Annie Liang[b], Eric Moore[b], Jacqueline Panigel[b], Mark Urban[b], Jixin Wang[b], Kerry Fillgrove[c], Cuyue Tang[c], Sean Cook[b], Stefanie Kane[b], Christopher Salvatore[b], Samuel Graham[a], Christopher Burgey[a]

[a] *Department of Medicinal Chemistry, MRL, Merck & Co., Inc., PO Box 4, West Point, PA 19486, USA*

[b] *Department of Pain Research, MRL, Merck & Co., Inc., PO Box 4, West Point, PA 19486, USA*

[c] *Department of Drug Metabolism, MRL, Merck & Co., Inc., PO Box 4, West Point, PA 19486, USA*

Abstract—A second-generation small molecule P2X3 receptor antagonist has been developed. The lead optimization strategy to address shortcomings of the first-generation preclinical lead compound is described herein. These studies were directed towards the identification and amelioration of preclinical hepatobiliary findings, reducing potential for drug-drug interactions, and decreasing the projected human dose of the first-generation lead.

Despite the presence of numerous treatment options, pain due to osteoarthritis is still a primary complaint of older populations; furthermore, only a small percentage of pain sufferers receive a prescription treatment. New drugs with minimal side effects, improved efficacy, and ease of administration are sought for the treatment of pain. The P2X3 receptor is an ATP-gated ion channel expressed on nociceptors (primary afferent neurons that sense painful stimuli) with limited receptor expression in other tissues.[1] Its role in the transmission of nociceptive stimuli along with its selective expression pattern makes the P2X3 receptor an attractive target with the potential to provide treatment of inflammatory, visceral, and neuropathic pain states.[2] Indeed, P2X3 receptor antagonists identified in our laboratories have already demonstrated dose-dependent reversal of pain in the rat Complete Freund's Adjuvant (CFA) assay.[3]

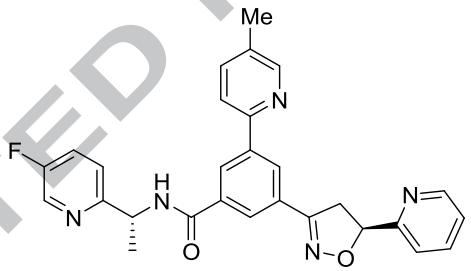

MK-3901

FLIPR IP = 21 nM
EP IC_{50} = 24 nM
Rat CFA: EC_{90} ~ 3 μM

CYP2C9 IC_{50} = 5.7 μM
PXR EC_{50} = 47% @ 10 μM
UGT1A1 IC_{50} = 1 μM

Rat Pharmacokinetics
%F = 60
PPB = 98.4%
$Cl_{int,\ in\ vivo}$ = 133 mL/min/kg
$t_{1/2}$ = 1.0 h

Predicted human dose:
420 mg TID

Figure 1. Profile of MK-3901.

MK-3901, disclosed previously, was the first P2X3 receptor antagonist preclinical candidate identified by our laboratories. MK-3901 is a potent antagonist of the P2X3

18 receptor as measured by our Ca^{++} mobilization FLIPR and patch clamp electrophysiology
19 (EP) assays (FLIPR IP = 21 nM, EP IC_{50} = 24 nM).[4] Importantly, when evaluated in the
20 rat CFA model of inflammatory pain, MK-3901 demonstrated efficacy similar to that of
21 our positive comparator, naproxen, after 60 mg/kg (p.o.) administration with a measured
22 EC_{90} of approximately 3 μM.[3] However, in non-human preclinical safety studies MK-
23 3901 was shown to induce hyperbilirubinemia across several species, most notably a
24 greater than 15-fold increase in total bilirubin levels in rhesus at exposures approximately
25 6-fold over the projected clinical AUC. The elevated bilirubin levels associated with
26 MK-3901 could potentially be attributed to off-target inhibition of UGT1A1 (IC_{50} = 1
27 μM), a glucuronosyltransferase involved in bilirubin metabolism.[4] MK-3901 exhibited
28 excellent bioavailability (%F) in rat, dog, and rhesus monkey pharmacokinetic (PK)
29 studies (F = 60%, 68%, and 47%, respectively), however the compound was found to be
30 extensively metabolized in human liver microsomes. Analysis of these metabolites
31 identified both the northern pyridine methyl group and the isoxazoline ring as metabolic
32 soft-spots. These factors lead to unacceptably high predicted dose and dose frequency
33 (420 mg TID). In addition to hepatobiliary findings and a high projected human dose,
34 MK-3901 also presented the potential for drug-drug interactions (DDI) due to
35 cytochrome P450 (CYP2C9) inhibition and pregnane X receptor (PXR) activation as
36 shown in Figure 1.
37
38 Using MK-3901 as a starting point, we sought to identify a second-generation potent and
39 selective P2X3 receptor antagonist with reduced risk of hyperbilirubinemia (through
40 attenuating off-target UGT1A1 inhibition) and reduced potential for DDI (through
41 minimized CYP inhibition/induction). We also targeted a lower projected clinical dose

through improved PK, and *in-vivo* potency in our rat CFA study. We describe herein the design and synthesis of potent P2X3 receptor antagonists which address these limitations.

The team took a modular approach to SAR exploration, examining the three substituent positions of the central benzene ring. We initially set out to replace the eastern isoxazoline side chain of MK-3901 to eliminate its metabolic liability and identify the minimum pharmacophore necessary for activity. Through incorporation of a wide variety of truncated eastern substituents (select examples are shown in Table 1), it was discovered that potency could be maintained while modulating plasma protein binding. Another advantage of investigating the minimum pharmacophore was that there appeared to be a correlation between eastern substituent size and UGT1A1 activity, with smaller substituents leading to reduced UGT1A1 inhibition across multiple structural series.[6] Unfortunately, incorporation of smaller eastern substituents led to higher in vivo plasma clearance in rat and dog; additionally,the risk for drug-drug interaction persisted for these compounds as CYP inhibition and PXR activation remained for many analogs. We were most encouraged by the tertiary-hydroxyl compound **4** which, despite lacking the entire pyridyl isoxazoline of MK-3901, lost only a modest amount of P2X3 potency, and displayed increased unbound fraction in rat plasma when compared with MK-3901.

Table 1. SAR of eastern substituents.

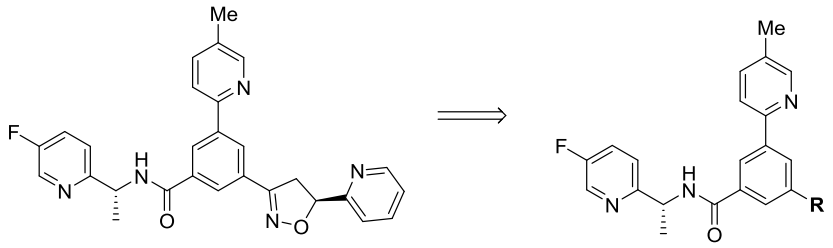

Compound	R	P2X3 FLIPR IP (nM)	$Cl_{int,\ in\ vivo}$ (mL/min/kg)[a]	PPB[a]	PXR EC_{50} (μM)
1		37	3911	97.4%	NA
2	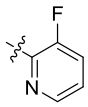	8	24780	99.2%	6
3		47	533	85.1%	>30
4		67	NA	82.0%	2

[a]values in rat

While SAR of the eastern portion of the molecule was ongoing, optimization of the western amide was being concomitantly investigated with the plan to combine the independent findings in both areas into a final optimized molecule. Utilization of the potency-enhancing eastern fluoropyridine present in compound **2** and varying the identity of the western amide led to a large class of compounds, representative examples of which are shown in Table 2. The team discovered early on in investigating western substituents that a variety of 5- and 6-membered aromatics and heterocycles were well tolerated in place of the western fluoropyridine of MK-3901. Another interesting finding was that the (*R*)-methyl substituent at the benzylic position in compounds **2-7**, **10** was preferred from

a binding perspective when compared with larger substituents (compound **13**), disubstitution (compound **12**) or the unsubstituted methylene (compounds **14**, **15**). One interesting exception to this trend is the triazole-containing compound **9**, where it has been rigorously confirmed that (*S*)-methyl stereochemistry is preferred.

Table 2. SAR of western amides

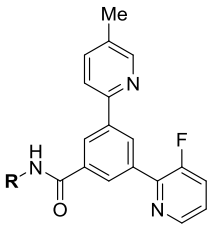

Compound	R	FLIPR IP (nM)	PPB (r)	Compound	R	FLIPR IP (nM)	PPB (r)
2	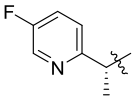	8	99.2%	**10**	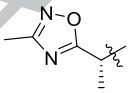	3	99.6%
5	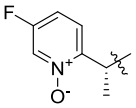	2	90.4%	**11**	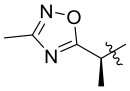	17	NA
6	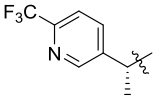	8	98.6%	**12**	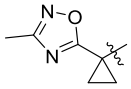	170	NA
7	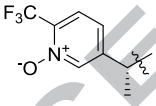	5	95.2%	**13**	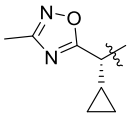	30	NA
8	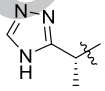	284	NA	**14**	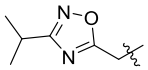	155	NA
9	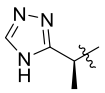	10	98.8%	**15**	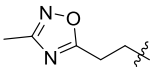	45	NA

Table 2 shows that while we had achieved potency below 10 nM in many cases, this class of eastern fluoropyridines continued to suffer from relatively high rat plasma protein

binding with the exception of the two pyridine *N*-oxide compounds, **5** and **7**. The team took particular interest in these amides which also showed substantially increased FLIPR potency.

Next, we then set forth to conjoin the independent SAR findings of the eastern and western regions into a single molecular entity. Indeed, as Figure 2 shows, when incorporated into the eastern tertiary hydroxyl scaffold, the pyridine *N*-oxide amide gives not only enhanced FLIPR potency and reduced plasma protein binding, but also reduced PXR activation and CYP inhibition when compared to its non-oxidized pyridine counterpart.

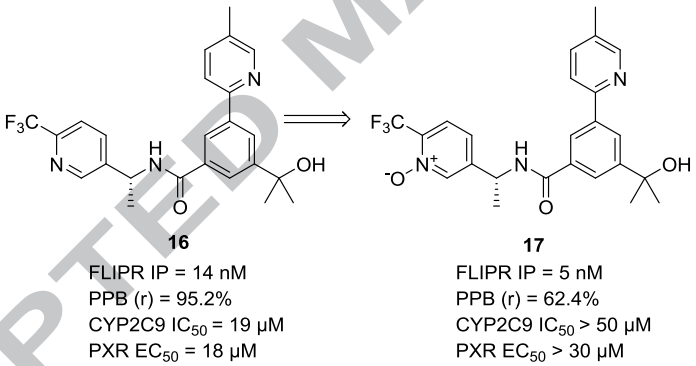

Figure 2. Advantages of Pyridine *N*-oxides

Having addressed the CYP inhibition/PXR activation and high plasma protein binding of MK-3901, the team focused on improving the pharmacokinetics of the potent and selective pyridine *N*-oxide antagonists. The methyl group of the northern pyridine ring had been identified as another site of oxidative metabolism by metabolite identification studies. As such, SAR exploration was conducted to find alternative northern rings with reduced metabolic potential.

Table 3. SAR of northern substituents

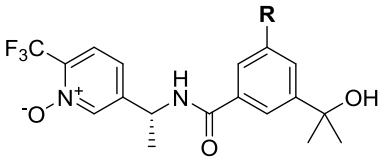

Compound	R	P2X3 FLIPR IP (nM)	PPB[a]	$Cl_{int,\ in\ vivo}$ (mL/min/kg)[a]	$t_{1/2}$ (h)[a]
17	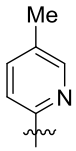	5	62.4%	NA	NA
18	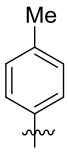	20	95.4%	6790	0.2
19	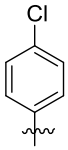	21	97.4%	214	2.4
20	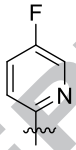	82	55.3%	477	0.48
21	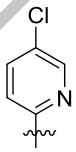	14	76.2%	69	1.3

[a] values in rat

As shown in Table 3, while aryl fluorine and chlorine substituents were well tolerated replacements for the metabolically labile methyl group of compound **17**, the

corresponding fluoropyridine analogs were found to significantly reduce FLIPR potency (compound **20**). Additionally, the fluoropyridines suffered from low exposures and short half-lives by nature of their high *in vivo* intrinsic clearance. Conversely, the northern chloropyridines, represented by compound **21** were found to have acceptable potency in the FLIPR assay to go along with increased exposure and lower intrinsic clearance. Additionally, compound **21** was subsequently shown to possess an exceptional off-target profile and increased *in vivo* potency in the rat CFA model of inflammatory pain (EC_{90} = 0.16 μM) when compared with MK-3901 (EC_{90} = 3 μM). Pertaining to the hyperbilirubinemia liability of MK-3901, compound **21** was found to display an IC_{50} of greater than 20 μM in the UGT1A1 inhibition assay. Lastly, compound **21** was predicted by allometric scaling to be a relatively low clearance (1.2 – 3.6 mL/min/kg) compound with a terminal half-life of 3 - 10 hr in humans, likely suitable for once daily dosing schedule.

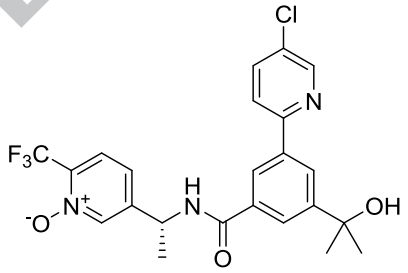

21

	Rat Pharmacokinetics	**Dog Pharmacokinetics**
FLIPR IP = 14 nM	%F = 13	%F = 63
EP IC_{50} = 18 nM	PPB = 76.2%	PPB = 73.7%
Rat CFA: EC_{90} = 160 nM	$Cl_{int,\ in\ vivo}$ = 69 mL/min/kg	$Cl_{int,\ in\ vivo}$ = 7.7 mL/min/kg
CYP2C9 IC_{50} = 82 μM	$t_{1/2}$ = 1.3 h	$t_{1/2}$ = 3.9 h
PXR EC_{50} > 30 μM		
UGT1A1 IC_{50} > 20 μM		

Figure 3. Profile of Compound 21.

The initial synthesis of compound **21** is shown in Scheme 1. Treatment of commercially available **22** with bis(pinacolato)diboron under standard Suzuki Conditions[7] results in selective cross-coupling with the iodide to give the boronic ester **23**. A second Suzuki reaction with 2-bromo-5-chloropyridine using water soluble triphenylphosphine conditions[8] gives the biphenyl product **24**. Here we observe a loss of desired product to subsequent cross-coupling of **24** with the starting boronate **23** leading to a modest 41% yield after 2 steps. A third cross-coupling with isopropenyl boronic ester yields the isopropenyl product **25**. After basic hydrolysis of the ester, a solvolysis reaction on the isoprene moiety in aqueous methanesulfonic acid gave the tertiary hydroxyl intermediate **26** in 59% yield after two steps. Completion of the sequence was affected through a standard amide coupling with amine **27** to give compound **21** in 16% overall yield in 6 steps.

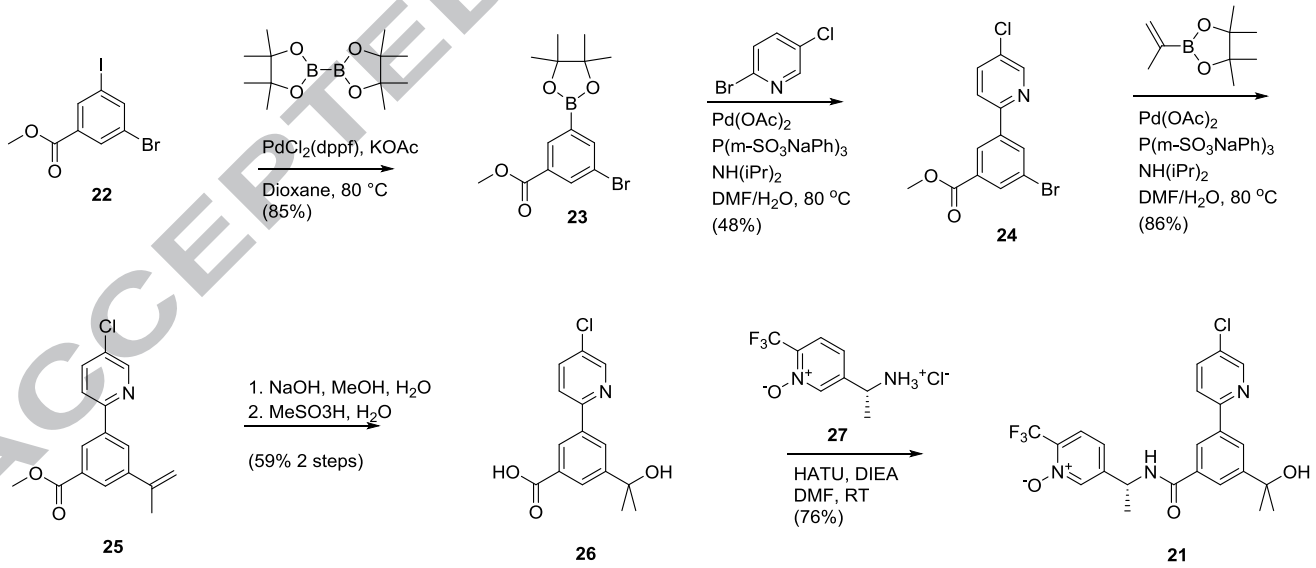

Scheme 1. Initial synthesis of Compound 21

In an attempt to increase the yield and efficiency of the initial route, we turned our attention to the first two Suzuki cross-coupling steps as areas for potential improvement. In a recent pair of publications[9,10] from our labs, it was demonstrated that copper (I) facilitates Suzuki reactions of historically challenging 2-heterocyclic boronates. Through the use of this methodology, the team was able to directly couple the chloropyridyl group to **22** thereby eliminating one of the cross-coupling steps from the route and increasing the overall yield more than 2 fold as shown in Scheme 2.

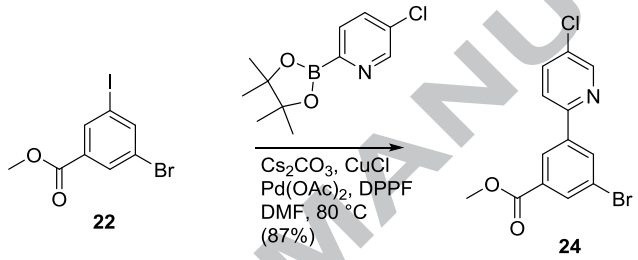

Scheme 2. Copper-facilitated Suzuki coupling to give intermediate 24.

In summary, we have taken a modular approach to lead optimization in identifying second-generation P2X3 receptor antagonists which address the issues observed in our first-generation preclinical candidate, MK-3901. We have sought to improve PK and *in vivo* potency in our preclinical pain model in an effort to reduce the predicted human dose. Truncation of the isoxazoline side chain of MK-3901 eliminated a metabolic liability present in the initial lead. Through incorporation of the pyridine *N*-oxide amide side chain, we were able to enhance both potency and free fraction. Replacement of the northern methylpyridine present in MK-3901 with chloropyridine gave compound **21** which not only displays the pharmacokinetic and physical properties to enable QD dosing, but also drives down unwanted off-target activities, namely UGT1A1 as well as

CYP inhibition and PXR activation. In addition to identifying an improved candidate molecule, we improved the synthetic efficiency of the first-generation synthesis of compound **21**.

References and notes

1. Bunstock, G. *Pharmacol. Ther.* **2006**, *110*, 433
2. Ford, A. P. *Pain Manage.* **2012**, *2*, 267
3. Burgey, C. *Abstracts of Papers*, 241st ACS National Meeting & Exposition, Anaheim, CA, Mar 27–31, 2011; American Chemical Society: Washington, DC, 1996; MEDI15.
4. Assay protocols for FLIPR, EP, CFA models as described in: Burgey, C. S.; Deng. Z. J.; Nguyen, D. N.; Paone, D. V.; Potteiger, C. M.; Vacca, J. P. WO Patent 058298 A1, 2009
5. Zhang D.; Chando, T; J.; Everett, D. W.; Patten, C. J.; Dehal, S. S.; Humphreys, W. G. *Drug. Metab. Dispos.* **2005**, *33*, 1729
6. Data not shown. As measured by inhibition of UGT1A1 catalyzed estradiol-3-glucuronidation in human liver microsomes.
7. Ali, A.; Bohn, J.; Deng, Q.; Lu, Z.; Sinclair, P. J.; Taylor, G. E.; Thompson, C. F.; Quraishi, N. WO Patent 100298 A1, 2005
8. Burgey, C. S.; Deng, Z. J.; Nguyen, D. N.; Paone, D. V.; Potteiger, C. M.; Stauffer, S. R.; Segerdell, C.; Nomland, A.; Lim, J. J. WO Patent 111058 A1, 2010
9. Deng, J. Z.; Paone, D. V.; Ginnetti, A. T.; Kurihara, H.; Dreher, S. D.; Weissman, S. A.; Stauffer, S. R.; Burgey, C. S. *Org. Lett.* **2009**, *11*, 345
10. Crowley, B. M.; Potteiger, C. M.; Deng, J. Z.; Prier, C. K.; Paone, D. V.; Burgey, C. S. *Tetrahedron Lett.* **2011**, *52*, 5055

Graphical Abstract

A second-generation small molecule P2X3 receptor antagonist has been developed. The lead optimization strategy to address shortcomings of the first-generation preclinical lead compound is described herein. These studies were directed towards the identification and amelioration of preclinical hepatobiliary findings, reducing potential for drug-drug interactions, and decreasing the projected human dose of the first-generation lead.

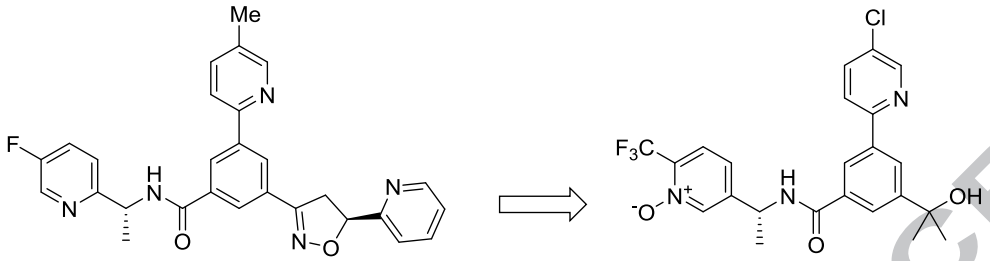

1st generation candidate
P2X3 FLIPR IP = 21 nM
UGT1A1 IC_{50} = 1 μM
CYP2C9 IC_{50} = 5.7 μM

21
P2X3 FLIPR IP = 14 nM
UGT1A1 IC_{50} > 20 μM
CYP2C9 IC_{50} = 82 μM